Optics Communications 434 (2019) 1–6

Contents lists available at ScienceDirect

Optics Communications

journal homepage: www.elsevier.com/locate/optcom

Analysis and correction of the distortion error in a DMD based scanning lithography system

Qian-Kun Li [a], Yao Xiao [a], Hua Liu [a,b,*], Hao-Lin Zhang [b,c], Jia Xu [b], Jin-Huan Li [a]

[a] Center for Advanced Optoelectronic Functional Materials Research, and Key Laboratory for UV-Emitting Materials and Technology of Ministry of Education, Northeast Normal University, 5268 Renmin Street, Changchun 130024, China

[b] State Key Laboratory of Applied Optics, Changchun Institute of Optics, Fine Mechanics and Physics, Chinese Academy of Sciences, Changchun 130033, China

[c] Departamento de Física, Universitat Autònoma de Barcelona, Bellaterra, 08193, Spain

ARTICLE INFO

Keywords:
Microlithography
Lithography
Digital image processing

ABSTRACT

DMD based lithography system provides the feasibility to achieve multi-point parallel direct writing exposure. However, the distortion of the projection lens in a scanning lithography system not only deviates the vertical size (vertical to the scanning direction), but also deviates the center position of an accumulated exposure point from the ideal one. In this work, we report a simple and realizable imaging compensation method, demonstrate as a combination of changing the magnification of the projection lens with loading an appropriately designed mask on DMD to eliminate the effects induced by distortion. With this method, the maximum center deviation of the accumulated exposure point is reduced from 4.3 μm to 1.45 μm, and the maximum size error is reduced from 0.4 μm to 0.1 μm with a 0.03% distortion projection lens in simulation. Moreover, we demonstrated the feasibility and effectiveness of the method experimentally by fabricating gratings with high geometry quality in large areas. Therefore, such simple method may have practical significance for improving the lithography quality of DMD-based system.

1. Introduction

Today, lithography techniques are indispensable in micro-fabrication because they provide the feasibility to fabricate light weight, integrated optoelectronic devices [1–4]. However, the difficulties in photomask fabrication and their high maintenance costs restrict the development of micro-processing technology. Under this scenario, numbers of maskless lithography technologies are proposed [5–10]. Among these technologies, DMD based digital lithography presents interesting benefits comparing with other alternatives. By introducing a DMD as a dynamic photomask (by selectively reflecting the incident light), DMD scanning lithography system is able to achieve multi-point parallel writing and large area processing [9,10]. In a DMD lithography system the high-resolution projection lens is one of the most important components, and its main function is to project the mask pattern onto the lithographic substrate with a certain magnification [11,12]. However, even though a large magnification can provide a high precision exposure, the distortion of the projection lens deteriorates the quality of the final exposure pattern. Moreover, it is difficult to design a projection lens that provides a wide field of view without distortion [13,14]. Under the circumstances, two main methods, described as using a complex spherical and a spherical lens contained optical system [15] or incorporating the camera distortion and the irregular illumination into the motion model [16] are proposed to eliminate the lithography pattern quality reduction introduced by the distortion. The first proposed method demands extremely high calibration precision, leads to the increase in the system cost; the second method requires a complex distortion transformation algorithm, which reduces the efficiency of the lithography process.

In this work, firstly, we studied the error of loading and adjusting of projection objective by ZEMAX. In actual installation, the manufacturing error and adjustment error of projection lens may introduce the distortion of the projection lens and further deteriorate lithography quality of DMD-based system. Then, we theoretically simulate the offsets of size and location of each accumulated exposure point from their desired value influenced by the distortion of the projection lens. To address this issue, we adopt increasing magnification of the photolithography lens to solve the problem of center aberration and use imaging compensation method (loading an appropriately designed mask) to reduce the size deviation of accumulated exposure point. With our method, the maximum center deviation is reduced from 4.3 μm to 1.45 μm, and the maximum size deviation is reduced from 0.4 μm to 0.1 μm with a 0.03% distortion projection lens in simulation. At last, we applied this correction method to the DMD based lithography experiment and obtained gratings with high geometry quality and surface quality.

* Corresponding author.
E-mail address: liuhua_rain@aliyun.com (H. Liu).

https://doi.org/10.1016/j.optcom.2018.10.042
Received 15 May 2018; Received in revised form 19 October 2018; Accepted 22 October 2018
Available online 26 October 2018

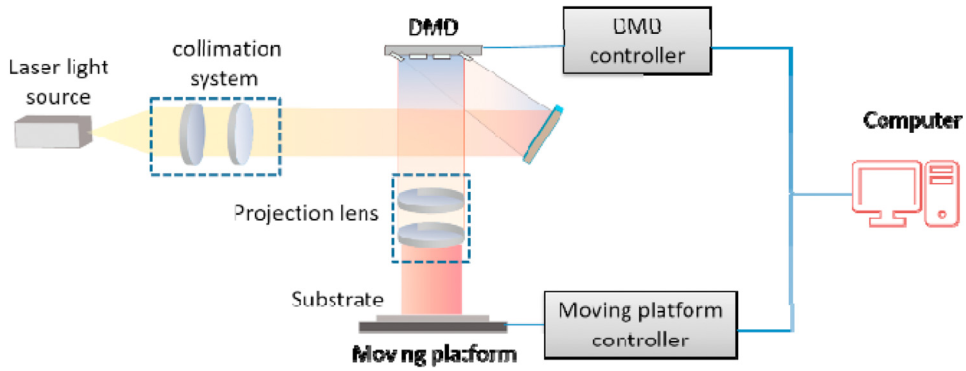

Fig. 1. Schematic illustration of DMD based lithography system.

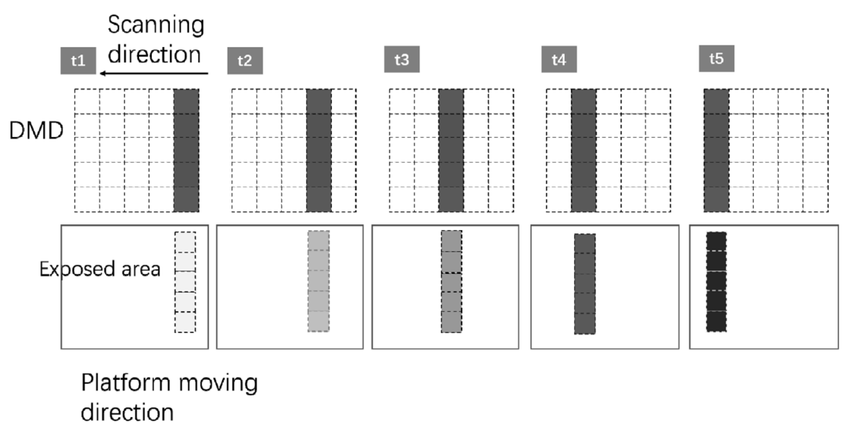

Fig. 2. Schematic illustration of lithography process of DMD based lithography system.

2. Experimental setup and theoretical simulations

2.1. Experimental setup

The four main parts of the DMD based lithography system [17] are the illuminating system: the DMD (spatial light modulator), the projection lens system, the illumination system, and the exposure platform. Fig. 1 shows the layout of the DMD based lithography system. The laser beam collimated by the collimation system and reflected to the DMD panel by a reflecting mirror first. Afterward, the light reflected from the DMD with digital lithography pattern is projected into the projection lens. The reflecting light carries the generated dynamic lithography pattern. Finally, the lithography pattern is projected to the substrate on the precision moving platform with a certain magnification.

A DMD (digital micromirror) is a reflective light modulator. It is consisted of numbers of micromirrors, each micromirror represents one pixel. When a micro-mirror generates a rotation of +12 degree, the illumination of this micro-mirror on the DMD is reflected into the projection lens and a bright pixel is formed on the photoresist substrate. When the micro mirror rotates a −12 degree, the light on the same point in the DMD is not reflected into the projection lens and a dark pixel is formed on the photoresist substrate, correspondingly.

Thus, the projection lens projects the graphical information created by the DMD onto the photoresist substrate, in the form of a quantized pattern with bright and dark pixels. In the real implementation, the moving platform is moving at a constant speed while the DMD device stands stationary. The graphic data are introduced into the DMD line by line to realize the scrolling update of the graph displayed in the DMD. All micro-mirrors in the DMD are flipped to form a corresponding frame with each line of data inputted. The principle of scanning lithography is demonstrated in Fig. 2 by a simple example with DMD consisting a 5×5 pixel mesh. The white pixels represent an "ON" status mirror, and the black pixels represent "OFF". The gray square corresponds to the exposed area, and the white square corresponds to the unexposed area. In step t1, the lithography pattern of a rectangular with 5 pixels in the first column is introduced into the DMD; the corresponding exposure pattern projected by the lens on the substrate is obtained with a certain exposure dose. Then, the next rectangular pattern with 5 pixels in the second column is introduced into the DMD. Meanwhile, the platform moves a distance of one projected pixel size with the same scroll direction, the corresponding exposure pattern on the substrate is reinforced with the same exposure dose as step t1. At last, the accumulated exposure point (the black rectangular in t5) on the substrate got the sum of energy of those "on" pixels along column in scanning direction.

2.2. Theoretical design and simulations

Assuming that a micromirrors array of $M \times N$ (M is the number of rows and N is the number of columns) is used in a DMD as shown in Fig. 3. We set the center of the DMD array as the coordinate origin, the scroll direction (scanning direction) as x direction, the direction which is perpendicular to the scroll direction as y direction. The magnification of the projection lens is β. So the size of the projected image of the every micromirror is βd.

DMD scanning exposure is equivalent to N pixels scanning at the same time. The total dose received by the accumulative exposure point on the substrate can be calculated by Eq. (1).

$$H_n = \sum_{m=-(M/2)}^{m=M/2} I_{mn}(x, y) \cdot T \, (m \neq 0, n \neq 0) \tag{1}$$

Here, T is the time for one micromirror scroll. I_{mn} is the irradiance at the substrate of a single micromirror. (x, y) is the coordinate of a certain

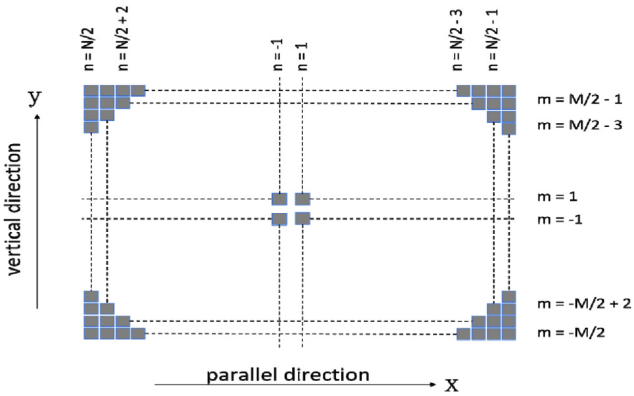

Fig. 3. Schematic illustration coded pattern of the DMD micro-mirrors.

image point. Due to the limitation of the lens, the irradiance is illustrated as a Gauss function shown as the following equation:

$$I_{mn}(x,y) = I_0 \cdot \exp\left\{-\left[\left(\frac{x}{a}\right)^2 + \left(\frac{y}{b}\right)^2\right]\right\} \tag{2}$$

Here, I_0 is the peak intensity of the pixel, a and b are the Gauss radii in two perpendicular directions. Actually, the lithography system works as the continuous scanning mode. Energy distribution of every pixel $I_{mn}(x,y)$ under scanning modes an integral of the energy distribution function of the corresponding micro-mirror under static mode when the stage is moving with time T. Therefore, the real exposure dose a single pixel receives is expressed as follow without considering the aberration of project lens:

$$I_{mn}(x,y) = \int_0^T I_0 \exp\left[\left(\frac{x+vt}{a}\right)^2 + \left(\frac{y}{b}\right)^2\right] d(t) \tag{3}$$

Here, v is the moving speed of the exposure platform, t is the exposure time. So the shape of the accumulated exposure point is an ellipse.

In fact, the project lens aberrations such as distortion also introduce an error causing the position of non-coincidence. The offset of a DMD pixel image from its ideal coordinate are expressed as $\Delta_{mn}x$ and $\Delta_{mn}y$ in two directions. The total dose received by the accumulate exposure point can be written as:

$$H_n(x,y) = \sum_{m=-(M/2)}^{x=M/2} \int_0^T I_{mn}\left(x+vt+\Delta_{mn}x,\right. \\ \left. y+\Delta_{mn}y\right) d(t)\, (m \neq 0, n \neq 0) \tag{4}$$

Considering the offset error, the non-coincidence of the central coordinate in X direction will result in the changing of the parallel size and the position, while the Y direction central coordinate non-coincidence changes the vertical size of the lithography pattern. For the sake of the deviation in X direction is mainly caused by the relative movement between the platform and the micromirror, the X offset error can be ignored, Eq. (4) can be written as Eq. (5):

$$H_n(x,y) = \sum_{m=-(M/2)}^{m=M/2} \int_0^T I_m\left(x+vt, y+\Delta_{mn}y\right) d(t)\, (m \neq 0, n \neq 0) \tag{5}$$

As one of the most critical components in a lithography system, the projection lens determines the image quality of the accumulated exposure points. What is more, the developing demands in micro-fabrication by using lithography technology not only prefer a high-resolution projection lens to achieve a high integration on the chip, but also require a small optical aberration to decrease the pattern aberration during the lithography process. However, considering the error appears in the fabrication of the lens used in the projection optical system and the error generated in the projection lens adjustment, a well performance projection lens is difficult to achieve. Under this scenario, the optical aberration, especially the optical distortion, will deteriorate the exposure pattern quality.

In this case, we mainly focus on the fabrication imprecision introduced by the optical distortion in the projection lens, represented as the radial displacement of the image point from its ideal paraxial position. Considering most optical systems share rotational symmetry structure, we establish a polar coordinate system in the imaging plane. In this case, the distortion of any point (l, θ) can be defined as Eq. (6) [18]:

$$q(l) = \frac{L-l}{l} \cdot 100\%. \tag{6}$$

Here, L represents the distance from any actual image point to the center of the coordinate system and l represents the distance from the ideal image point to the center of the field of view. In fact, the distortion, demonstrated in a polynomial, can be described as:

$$\mathrm{q}(l) = a_1 l^2 + a_2 l^4 + a_3 l^6 + \cdots, \tag{7}$$

Here, $a_1, a_2, a_3\ldots\ldots$ is the distortion coefficient. The quadratic function can satisfy the experimental requirements, so Eq. (7) can be written as:

$$q(l) = a_1 l^2 \tag{8}$$

The absolute distortion is defined as Δl, so the absolute distortion in the polar coordinate can be written as:

$$\Delta l = a_1 \cdot l^3 \tag{9}$$

In order to obtain the offset of the accumulate exposure point in the vertical direction (represented as Δ_{mn}), the coordinate transformation should be applied from the polar coordinate to the Cartesian coordinate.

$$\Delta_{mn} = \Delta l \cdot \cos\theta. \tag{10}$$

According to the rows and columns of the image point corresponds to each micromirror as coded in Fig. 3, l and θ can be expressed as:

$$l = \left(m^2+n^2\right)^{1/2} \cdot \beta \cdot d, \tag{11}$$

$$\cos\theta = \frac{n}{\sqrt{m^2+n^2}}. \tag{12}$$

Here, m and n are the row and column corresponding to the accumulate exposure point, β is the magnification of the projection lens. In this case, the offset of a single micromirror image in the vertical direction can be described as:

$$\Delta_{mn} = a_1\left(m^2+n^2\right) \cdot n \cdot \beta^3 \cdot d^3. \tag{13}$$

By introducing Eq. (5), the distribution of the exposure dose received by any accumulated exposure point, can be obtained. Due to the optical distortion existing in the projection lens, a central offset is appeared in the accumulated exposure point. In fact, not only the central coordinate, but also the image vertical size appears a deviation between the ideal pattern and the distortion contained pattern. In this case, the above-mentioned deviations directly reduce the accuracy and the consistency of the accumulated exposure points. Hence, in order to improve the central coordinate offset, a method described as changing the magnification of the projection lens, is proposed. When the change of the magnification of the projection lens is $\Delta\beta$, a vertical offset of a micro-mirror image point Δy_β is generated. It can be described as:

$$\Delta y_\beta = \Delta\beta \cdot l \cdot \cos\theta. \tag{14}$$

Considering Eq. (11) and Eq. (12), the vertical offset Δy_β can be given as:

$$\Delta y_\beta = n \cdot \Delta\beta \cdot d. \tag{15}$$

The distortion introduced by the projection lens generates a central position offset in the accumulated exposure point. The offset is demonstrated in Eq. (13). What is more, more central position offset of the

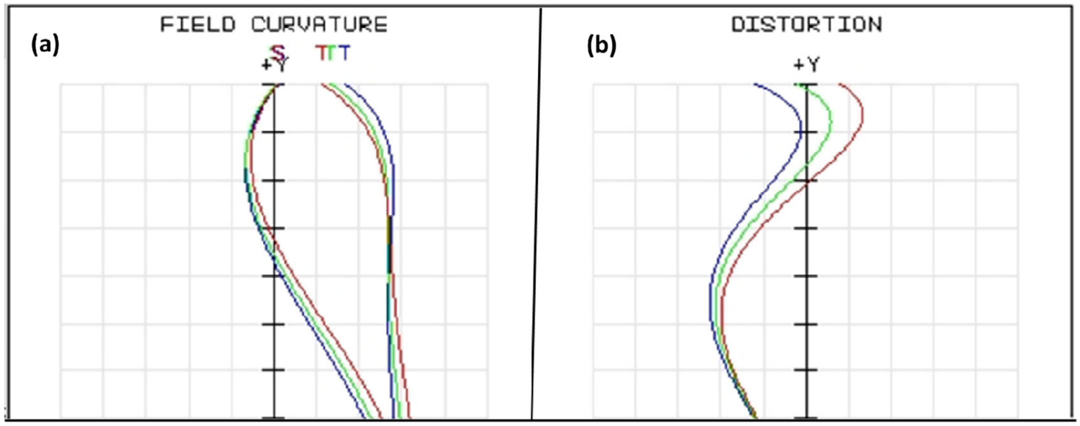

Fig. 4. (a) The distortion curve in the ideal situation (b) The distortion curve with considering the errors.

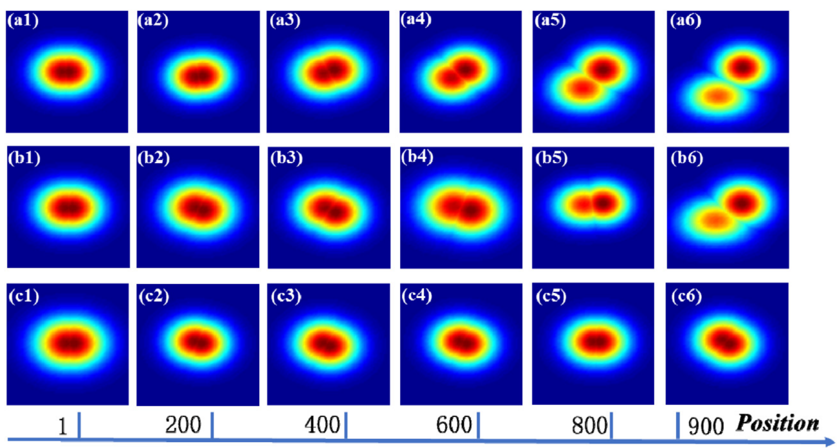

Fig. 5. (a1)–(a6) The calculated results of the exposure position relative to the ideal position before being corrected; (b1)–(b6) after increasing the magnification; (c1)–(c6) after increase the magnification and loading the special mask.

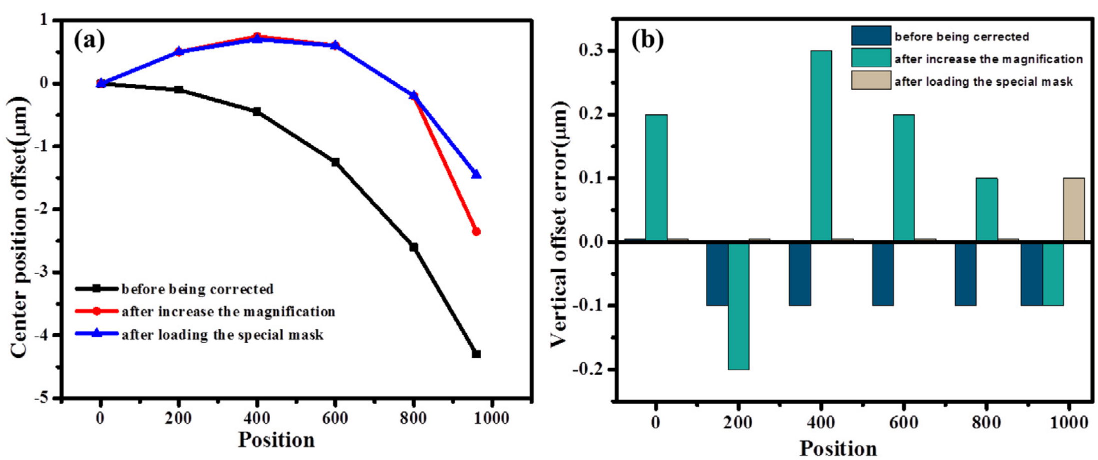

Fig. 6. (a) Center position offsets after increase the magnification and loading the special mask by simulation; (b) Vertical position offsets after increase the magnification and loading the special mask by simulation.

accumulated exposure point is introduced by changing the magnification of the projection lens. The corresponding offset is demonstrated in Eq. (15). Note that the total central offset in any accumulated exposure point is influenced by the two above-mentioned offsets. Hence, the final vertical offset of each micromirror image point is shown as follow:

$$\Delta y = \Delta_{nm} + \Delta y_{\beta} = a_1 \left(m^2 + n^2\right) \cdot n \cdot \beta^3 \cdot d^3 + \Delta\beta \cdot n \cdot d. \tag{16}$$

According to Eq. (16), for a certain distortion, the vertical offset can be reduced by selecting an appropriate magnification. Thereby, we can obtain an optimized offset of each micromirror image point and improve the center position error of the accumulated exposure point by changing the projector magnification.

However, this method can be hardly applied to correct the size of the accumulated exposure point, especially its vertical size. So we propose another method to correct it by loading an appropriately designed mask. The mask patten can make some micro-mirrors in each column turned off forever. So the energy of the accumulated exposure point is reduced to ensure its ideal size.

In order to maintain an invariable magnification during the lithography system calibration and the focusing process, a double-sided telecentric lens which provides a 1x magnification with the working wavelength ranges from 403 nm–407 nm, is employed as the projection lens. The projection lens proposed is simulated by Zemax, the distortion curve is represented in Fig. 4(a), which is almost zero in the whole aperture. However, in the real implementation, the lens fabrication error and the adjustment error will introduce a distortion into the projection lens, lead to a reduction in the lithography pattern quality. The distortion curve with considering the errors is shown in Fig. 4(b), the maximum distortion is 0.03%. An unpleasant distortion deterioration, which leads to a quality reduction in the exposure pattern, is presented from the comparison between the two distortion curves.

The least squares method is used to fit the distortion data, according to Eq. (8), the distortion of the projection lens is given as:

$$q(l) = -5 * 10^{-8} l^2 \tag{17}$$

The DMD implemented in the lithography system, containing a 1920 $*$ 1080 micromirrors array with a micromirror size of 10.8 μm, is provided by Texas Instruments. As shown in Fig. 3, the number of the DMD micromirror array row is numbered m, ranging from −960 to 960; the numbered of the DMD micromirror column array is n, ranging from −540 to 540. By considering Eqs. (5) and (16), the total dose received by the cumulative exposure points can be given as:

$$H_n = {}^1\!/_v \cdot \sum_{-(M/2)}^{(M/2)} \int_0^L I_0 \cdot \exp\Big(-\Big\{\big[{}^{(x+\Delta L)}\!/_a\big]^2 + \big[\big(y + a_1\left(m^2+n^2\right)\cdot n \cdot d \quad + \Delta\beta \cdot n \cdot d\big)\cdot b^{-1}\big]\Big\}\Big) \quad (m \neq 0, n \neq 0) \tag{18}$$

Based on Eq. (18), the energy distribution of each accumulated exposure point by considering the distortion can be simulated. Therefore, the center coordinate and the vertical size of the corresponding accumulate exposure point can be calculated. Fig. 5 (a1)–(a6) show simulation results of the exposure position relative to the ideal position before being corrected, it is obvious that the exposure deviation becomes greater when the further away from the center position. In order to decrease the deviation, we first adopt the method of increasing the magnifications of the projection lens and the calculated results were shown in Fig. 5 (b1)–(b6), center position offsets got a significant reduction meanwhile vertical position offsets did not decrease obviously. Hence, we introduce another error compensation method by loading the designed special mask to further reduce the vertical error, Fig. 5 (c1)–(c6) show that center position offset and vertical position offsets both have been corrected after increase the magnification and loading the special mask.

Fig. 6(a) and (b) show the tangible changed values of center position offsets and vertical position offsets after increase the magnification and loading the special mask by simulation. Before being corrected the center position offset at 900th exposure pixel is 4.3 μm, after increase the magnification and loading the special mask the center position offset at 900th exposure pixel is down to 1.45 μm. And the maximum vertical position offsets is reduced from 0.1 μm to near 0 with a 0.03% distortion projection lens in simulation.

Shown in Fig. 7 is our designed lithography mask which contains 1920 $*$ 1080 pixels (corresponding to the DMD micromirror array). Here, we first encode the micromirror array in the DMD, then simulate the corresponding intensity distribution of a column of micro-mirrors, then simulate the corresponding intensity distribution after shutting down part of the micro-mirrors; continually optimize the number and location of closed micro-mirrors until center position offsets and vertical position offsets of the column micro-mirrors are corrected. The black area, which refers to the DMD micromirrors with the "OFF" status, reflects no exposure light to the substrate and provides no exposure dose. DMD based lithography system will lose a little bit of the laser energy when add this mask, but this does not affect overall processing efficiency.

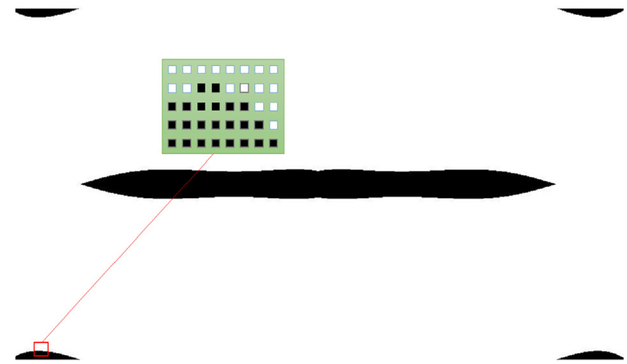

Fig. 7. Designed dynamic lithography mask.

3. Experimental results

In the front we have carried out theoretical simulation of the error compensation of DMD based lithography system, the errors can be effective eliminated by increasing the magnification of the projection lens and loading an appropriately designed mask on DMD. At last, we fabricated gratings using DMD scanning lithography assist with our error compensation method. Here, a laser with a wavelength of 405 nm is chosen as the light source, and a projection lens with a magnification of one is used as the projector, the scanning speed of the moving platform was 20 mm/s, the SU8 photoresist coated on the substrate is used as the photosensitive material. Fig. 8(a) and (b) are optical microscope photos of fabricated gratings in the center position and farthest away from the center position, respectively. Gratings in the area of center position exhibit excellent consistency and uniformity of cycles. Fig. 8 (b) shows gratings fabricated without error corrected and with error corrected using increasing the magnification of the projection lens and loading designed mask, it is obvious that gratings have shifted to the center position by about 3 μm after error compensation compared with gratings fabricated without error corrected. The experimental results are in agreement with the simulations that the center position offset at 900th exposure from 4.3 μm down to 1.45 μm after error corrected using the imaging compensation method. Gratings will remain uniform in large areas after error compensation indicating the effectiveness of our error compensation method. The experiments did not show vertical position offsets because it was too small. Both experimental and theoretical results show the effectiveness of our method for improving the lithography quality of DMD-based system, our method may also have referential value in the field of liquid crystal spatial light modulator (SLM) based systems because the similar way of controlling light [19,20].

4. Conclusion

In this paper, the exposure errors introduced by the projection lens distortion in a DMD based lithography system, was studied first. A method to eliminate the errors, demonstrated as the combination of increasing the magnification of the projection lens with loading an appropriately designed mask on DMD, was provided afterward. By increase the magnification of the projection lens by 0.00023, the center position of the accumulated exposure point was well corrected. However, the size of the accumulate exposure point was not significantly enhanced by introducing this method. Furthermore, we corrected the vertical size of the accumulate exposure point by loading a software mask. The simulation results proved that the maximum central offset can be reduced from 4.3 μm to 1.45 μm, and the maximum size error can be reduced from 0.4 μm to 0.1 μm. Finally, we demonstrated effectiveness of the error compensation method experimentally by fabricating gratings with high consistency and uniformity in large areas. Our method could be used for improving the lithography quality of DMD-based system.

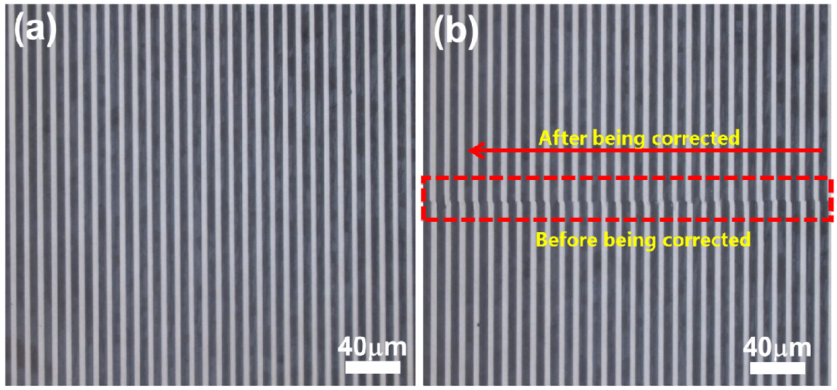

Fig. 8. Optical microscope photos of fabricated gratings. (a) Area in the center position. (b) Area farthest away from the center position.

Acknowledgments

The work described in this paper is supported by the National Natural Science Foundation of China under grant 61875036, Projects of Science and Technology Development Plan of Jilin Province, China and the State Key Laboratory of Applied Optics.

References

[1] T. Ito, S. Okazaki, Pushing the limits of lithography, Nature 406 (2000) 1027.
[2] R. Garcia, A.W. Knoll, E. Riedo, Advanced scanning probe lithography, Nature Nanotechnol. 9 (2014) 577–587.
[3] H. Kim, J. Ge, J. Kim, S.E. Choi, H. Lee, H. Lee, W. Park, Y. Yin, S. Kwon, Structural colour printing using a magnetically tunable and lithographically fixable photonic crystal, Nature Photon. 3 (2009) 534–540.
[4] S.K. Selvaraja, P. Jaenen, W. Bogaerts, D. Van Thourhout, P. Dumon, R. Baets, Fabrication of photonic wire and crystal circuits in silicon-on-insulator using 193-nm optical lithography, J. Lightwave Technol. 27 (2009) 4076–4083.
[5] A.P. Zhang, X. Qu, P. Soman, K.C. Hribar, J.W. Lee, S. Chen, S. He, Rapid fabrication of complex 3D extracellular microenvironments by dynamic optical projection stereolithography, Adv. Mater. 24 (2012) 4266–4270.
[6] L. Wang, B.B. Xu, Q.D. Chen, Z.C. Ma, R. Zhang, Q.X. Liu, H.B. Sun, Maskless laser tailoring of conical pillar arrays for antireflective biomimetic surfaces, Opt. Lett. 36 (2011) 3305–3307.
[7] Z.Y. Zhang, C.C. Zhang, Y.L. Hu, C.W. Wang, J.W. Li, Y.H. Su, J.R. Chu, D. Wu, Highly uniform parallel microfabrication using a large numerical aperture system, Appl. Phys. Lett. 109 (2016) 021109.
[8] O. Tokel, A. Turnali, G. Makey, P. Elahi, T. Çolakoğlu, E. Ergeçen, A. Bek, et al., In-chip microstructures and photonic devices fabricated by nonlinear laser lithography deep inside silicon, Nature Photon. 11 (2017) 639–645.
[9] S.H. Song, K. Kim, S.E. Choi, S. Han, H.S. Lee, S. Kwon, W. Park, Fine-tuned grayscale optofluidic maskless lithography for three-dimensional freeform shape microstructure fabrication, Opt. Lett. 39 (2014) 5162–5165.
[10] H. Wu, W. Hu, H.C. Hu, X.W. Lin, G. Zhu, J.W. Choi, V. Chigrinov, Y.Q. Lu, Arbitrary photo-patterning in liquid crystal alignments using DMD based lithography system, Opt. Express 20 (2012) 16684–16689.
[11] R.H. Chen, H. Liu, H.L. Zhang, W.J. Zhang, J. Xu, W.B. Xu, J.H. Li, Edge smoothness enhancement in DMD scanning lithography system based on a wobulation technique, Opt. Express 25 (2017) 21958–21968.
[12] M.P. Lee, M, G.J. Cooper, T. Hinkley, G.M. Gibson, M.J. Padgett, L. Cronin, Development of a 3D printer using scanning projection stereolithography, Sci. Rep. 5 (2015) 9875.
[13] K.F. Chan, W. Mei, Surface distortion compensated photolithography, U.S. Patent Application. 10/035, 2003, 387.
[14] D.H. Lee, Optical system with 4 μm resolution for maskless lithography using digital micromirror device, J. Opt. Soc. Korea 14 (2010) 266–276.
[15] T. Matsuyama, Y. Ohmura, D.M. Williamson, The lithographic lens: its history and evolution, Proc. SPIE 6154 (2006) 615403.
[16] Y. Altunbasak, R.M. Mersereau, A.J. Patti, A fast parametric motion estimation algorithm with illumination and lens distortion correction, IEEE Trans. Image Process. 12 (2003) 395–408.
[17] T.N. Ng, R.A. Lujan, S. Sambandan, R.A. Street, S. Limb, W.S. Wong, Low temperature a-Si: H photodiodes and flexible image sensor arrays patterned by digital lithography, Appl. Phys. Lett. 91 (2007) 063505.
[18] L.R. Baker, Aberrations of optical systems, J. Modern Opt. 34 (2007).
[19] C.C. Zhang, Y.L. Hu, J.W. Li, Z.X. Lao, J.C. Ni, J.R. Chu, W.H. Huang, D. Wu, An improved multi-exposure approach for high quality holographic femtosecond laser patterning, Appl. Phys. Lett. 105 (2014) 221104.
[20] J.C. Ni, Z.Y. Wang, Z.Q. Li, Z.X. Lao, Y.L. Hu, S.Y. Ji, B. Hu, C.C. Zhang, J.W. Li, D. Wu, J.R. Chu, Multifurcate assembly of slanted micropillars fabricated by superposition of optical vortices and application in high-efficiency trapping microparticles, Adv. Funct. Mater. 27 (2017) 1701939.